Author's personal copy

BRAIN RESEARCH 1305 (2009) 96–107

available at www.sciencedirect.com

ScienceDirect

www.elsevier.com/locate/brainres

BRAIN RESEARCH

Research Report

Frontoparietal activity and its structural connectivity in binocular rivalry

Juliane C. Wilcke[a,b,*], *Robert P. O'Shea*[c,d], *Richard Watts*[b,e]

[a]*Department of Psychology, University of Canterbury, Christchurch, New Zealand*
[b]*Department of Physics and Astronomy, University of Canterbury, Christchurch, New Zealand*
[c]*Department of Psychology, University of Otago, Dunedin, New Zealand*
[d]*Psychology, School of Health and Human Sciences, Southern Cross University, Coffs Harbour, NSW, Australia*
[e]*Van der Veer Institute for Parkinson's and Brain Research, Christchurch, New Zealand*

ARTICLE INFO

Article history:
Accepted 20 September 2009
Available online 25 September 2009

Keywords:
Visual awareness
Conscious perception
Binocular rivalry
Binocular fusion
fMRI
DTI tractography

ABSTRACT

To understand the brain areas associated with visual awareness and their anatomical interconnections, we studied binocular rivalry with functional magnetic resonance imaging (fMRI) and diffusion tensor imaging (DTI). Binocular rivalry occurs when one image is viewed by one eye and a different image by the other; it is experienced as perceptual alternations between the two images. Our first experiment addressed problems with a popular comparison condition, namely permanent suppression, by comparing rivalry with binocular fusion instead. We found an increased fMRI signal in right frontal, parietal, and occipital regions during rivalry viewing. The pattern of neural activity differed from findings of permanent suppression comparisons, except for adjacent activity in the right superior parietal lobule. This location was near fMRI signal changes related to reported rivalry alternations in our second experiment, indicating that neighbouring areas in the right parietal cortex may be involved in different components of rivalry. In our second experiment, we used probabilistic tractography to detect white matter fibres between right-hemispheric areas that showed event-related fMRI signal changes time-locked to reported perceptual alternations during rivalry viewing. Most of these functionally defined areas were linked by probabilistic fibre tracts, some of which followed long-distance connections such as the inferior occipitofrontal fasciculus. Corresponding anatomical pathways might mediate communication within the functional network associated with changes in conscious perception during binocular rivalry.

© 2009 Elsevier B.V. All rights reserved.

1. Introduction

When our left eye's view is incompatible with our right eye's view, we experience a remarkable phenomenon of visual awareness: binocular rivalry. Rather than seeing both views, we see one eye's view with no trace of the other's; a few moments later this changes so we see the other eye's view with no trace of the first's. Because binocular rivalry involves changes in visual consciousness without any change in the images viewed by the eyes, it has become a popular phenomenon for exploring the neural correlates of consciousness (Blake and Logothetis, 2002; Crick and Koch, 1990).

* *Corresponding author*. Department of Psychology, University of Canterbury, Private Bag 4800, Christchurch 8140, New Zealand. Fax: +64 3 364 2181.
E-mail address: juliane.wilcke@gmail.com (J.C. Wilcke).

0006-8993/$ – see front matter © 2009 Elsevier B.V. All rights reserved.
doi:10.1016/j.brainres.2009.09.080

Author's personal copy

Research on the brain areas involved in binocular rivalry in humans has mainly used functional magnetic resonance imaging (fMRI) to measure changes in the flow of oxygenated blood in the brain while a person is experiencing binocular rivalry. This research has shown activity changes associated with observers' reported perception during rivalry, as indicated by the blood-oxygenation-level-dependent (BOLD) signal, at all stages of human visual processing: from the lateral geniculate nucleus (Haynes et al., 2005; Wunderlich et al., 2005), through the primary visual cortex (e.g., Lee et al., 2005; Polonsky et al., 2000; Tong and Engel, 2001), to dorsal and ventral higher visual areas, including object-selective areas such as the fusiform face area (e.g., Tong et al., 1998). In addition to visual cortex, the BOLD signal in frontal and parietal areas has also been found to correlate with perception during binocular rivalry (e.g., Lumer et al., 1998; Lumer and Rees, 1999). It is this rivalry-related activity in frontoparietal regions that is our interest in this paper.

A popular comparison condition for binocular rivalry (e.g., Lumer et al., 1998; Polonsky et al., 2000; Sterzer and Rees, 2008; Tong et al., 1998) simulates periods of exclusive visibility of one image, interspersed with perceptual alternations, to elicit a similar conscious perception to that of rivalry. This comparison condition is typically called *stimulus* or *physical alternation*, *nonrivalry*, or *replay*. Instead of showing one image to one eye and a different image to the other eye, the replay condition consists of showing one image to one eye and a uniform field, such as a homogeneous background, to the other eye. Perceptual alternations are achieved by physically changing the images to the two eyes. In both conditions, observers normally press keys to report their conscious perception of one and the other images. But O'Shea and Corballis (2005a) pointed out two problems with this procedure. First, because a contoured stimulus usually dominates a uniform field, the replay condition involves a form of rivalry too, known as *permanent suppression* (Hering, 1964; Ooi and Loop, 1994). So any comparison is between two forms of rivalry. Second, the judgements of perceptual changes during rivalry are much more difficult than during the replay condition. So any comparison is between difficult and easy judgements.

To address the first problem, we created a comparison condition that did not involve permanent suppression, by presenting identical stimuli to the observer's two eyes. When our eyes' views are congruent, we see a single image from fusion of the two. Our *fusion* stimuli differed from the rivalry stimuli only in the desired absence of perceptual competition, achieved through removing the rivalry-inducing difference in orientation. We illustrate the stimuli used in our experiments in Fig. 1. When we compared the viewing of rivalry stimuli with that of fusion stimuli, we found an increased BOLD signal in frontal, parietal, and occipital areas.

To address the second problem, namely the difference in difficulty between perceptual change judgements in rivalry and in existing replay conditions, one would need to create a nonrival display that is perceptually indistinguishable from a rival display. To our knowledge, no such display has been realised. We went some way towards controlling for the differences in difficulty by asking participants simply to observe rival and fusion stimuli without pressing any keys. Lumer and Rees (1999) analysed passive rivalry viewing by itself and found activity in frontoparietal cortex that covaried with activity in an extrastriate area identified by Lumer et al. (1998) as an indicator of reported rivalry alternations. Our comparison of rivalry and fusion viewing, which was independent of current and past key presses, provides additional support for the association of frontoparietal activity with binocular rivalry.

Our other major concern was to explore white matter connections among brain areas whose activity is related to perceptual alternations during binocular rivalry. The investigation of the neuroanatomical pathways that communicate signals between distant brain regions involved in the generation of visual consciousness is an important avenue for research into the biological bases of consciousness (Crick and Koch, 1998; Rees et al., 2002; Roser and Gazzaniga, 2004). For example, two influential neurobiological theories of consciousness (Dehaene and Naccache, 2001; Dehaene et al., 2006; Lamme, 2003, 2006) require connectivity between posterior and anterior regions in the brain, particularly between visual areas and frontoparietal cortex, for conscious access to visual information. Because there is no consensus yet on the specific locations of frontoparietal areas associated with binocular rivalry alternations, we studied anatomical connections between the brain areas that showed event-related activity to reported rivalry alternations in individual observers.

To detect fibre tracts between areas associated with rivalry alternations, we employed a combination of fMRI and diffusion

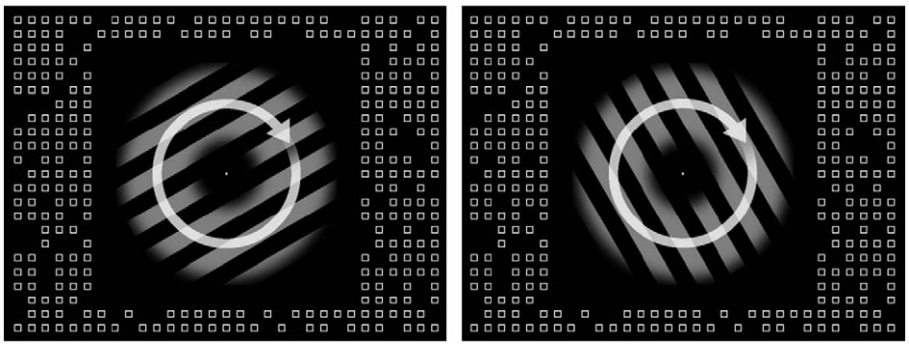

Fig. 1 – Example of binocular rivalry stimuli. Participants observed the left panel stimulus with one eye and the right panel stimulus with the other eye. In Experiment 1 such rivalry periods alternated with periods of binocular fusion, in which the two gratings were identical in orientation. Both gratings presented in Experiment 1 were green; in Experiment 2 one was green and the other red. The arrows indicate continuous clockwise rotation of each grating.

Author's personal copy

Table 1 – Brain areas with higher BOLD signal during binocular rivalry than during binocular fusion viewing.

Anatomical label	x	y	z	t	% change (SE)	Vox.
Superior parietal lobule	30	-49	48	12.6	0.268 (0.021)	25
Precentral gyrus	56	0	40	11.3	0.204 (0.018)	4
Hippocampus	-26	-41	4	10.6	0.059 (0.006)	3
Median cingulate and paracingulate gyri	22	-41	32	9.9	0.036 (0.004)	4
Precuneus	22	-41	8	7.7	0.052 (0.007)	1
Middle frontal gyrus	34	-4	56	7.1	0.210 (0.030)	2
Superior occipital gyrus	26	-86	24	6.1	0.342 (0.056)	1

Results are from a mixed-effects group analysis, $t(5)=5.89$, $p<0.001$, uncorrected (cf. FWE-corrected fixed-effects group results in the text). All data, except for those in the last column, refer to a cluster's maximum voxel. Coordinates in millimetres are in MNI space. % change = estimated percent change of global mean signal associated with the contrast *rivalry > fusion*; SE = standard error; vox. = number of above-threshold voxels in the cluster.

tensor imaging, which uses water motion to infer the orientation of white matter bundles throughout the brain. We first identified BOLD signal foci associated with reported rivalry alternations in each observer and then noninvasively traced connections between these areas in the right hemisphere. This was possible through the use of a novel probabilistic tractography technique that can follow tracts in grey matter and in areas of crossing fibres. Almost all areas of event-related BOLD signal, whose locations at the group level were consistent with previous findings of rivalry-alternation activity (e.g., Lumer et al., 1998), were linked by probabilistic fibre tracts.

2. Results

2.1. *Experiment 1: Comparison of binocular rivalry with binocular fusion*

In Experiment 1, six participants observed alternating 30-s blocks of binocular rivalry and fusion; they were instructed only to look at a fixation point in the centre of the stimuli. Our mixed-effects analysis of their functional imaging data suggested that frontal, parietal, occipital, and limbic areas had a higher BOLD signal during rivalry viewing than during fusion viewing, $t(5)=5.89$, $p<0.001$, uncorrected for multiple comparisons across 22 515 voxels (22.5 voxels expected to be false positives; see Fig. 2 and Table 1). All of the signal maxima, except for the hippocampal maximum, were in the right hemisphere. The two cluster maxima with the highest t values were located in the superior parietal lobule and the precentral gyrus (see Supplementary Fig. 1 for unthresholded axial maps of individual and group results). The size of the parietal cluster made it unlikely to be a chance discovery, cluster-level inference, 25 voxels, $p=0.0003$, corrected.

Average BOLD signal increases in the maximum voxels in the middle frontal, precentral, superior parietal, and superior occipital regions were 0.20–0.34% of the global mean signal; those in two limbic regions and the precuneus were only 0.04–0.06%. The maximum voxels in the former four regions were also statistically significant in the mean results of our

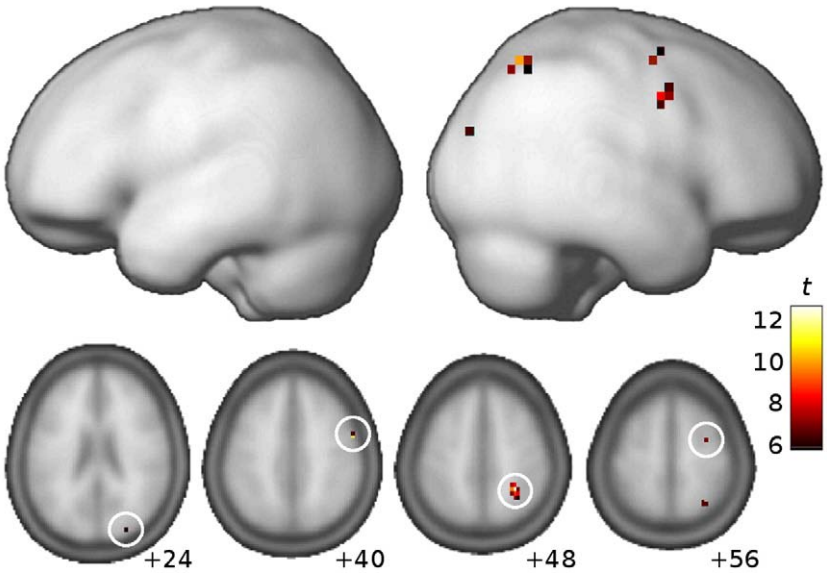

Fig. 2 – Brain areas with higher BOLD signal during binocular rivalry than during binocular fusion viewing. The results of a mixed-effects analysis ($t[5]=5.89$, $p<0.001$, uncorrected) are superimposed on the ICBM-152 T_1 template (top row: within 20 mm of the brain surface). Axial slices show above-threshold voxels in the right superior occipital gyrus (z = +24 mm), in the precentral gyrus (z = +40 mm), in the superior parietal lobule (z = +48 mm), and in the middle frontal gyrus (z = +56 mm).

Author's personal copy

participants, or had at least a neighbouring voxel that was so (fixed-effects group analysis), $t(1408)=5.35$, $p<0.001$, corrected for multiple comparisons by controlling the familywise error (FWE) rate (1 false positive expected in 1000 such studies). There were no voxels with a higher BOLD signal during fusion than during rivalry in the mixed-effects analysis.

In summary, viewing binocular-rivalry instead of binocular-fusion stimuli tends to increase BOLD signal in right parietal and frontal cortex, among other areas. The signal increases cannot be attributed to the planning and execution of key presses because the observers did not press any keys during imaging, nor can they be attributed to a difference in the difficulty of judgements because the observers were not asked to make any. Before discussing the identified regions within the context of other findings, we describe Experiment 2, in which we explored the structural connectivity between those cortical areas that showed BOLD signal fluctuations associated with rivalry alternations.

2.2. *Experiment 2: Anatomical links between rivalry-alternation areas*

2.2.1. *Behaviour*

The three participants in Experiment 2, VN, JM, and GH, observed binocular rivalry stimuli and reported their conscious perception of the red and the green grating by pressing keys with their right hands. The mean durations between reported perceptual alternations from one rivalry stimulus to the other were 5.0, 7.7, and 7.2 s, respectively, sufficiently long to elicit many discernible haemodynamic responses and to allow at least partial signal recovery between perceptual alternations (cf. Tong et al., 1998; Wunderlich et al., 2005). Alternations lasted on average 0.3, 0.4, and 0.2 s, respectively. By *alternation* we mean any period during which an observer held down both keys to report mixed perception and which was flanked by different single-key presses of any duration, indicating a change in the exclusively perceived image.

2.2.2. *Functional imaging*

A group analysis of the fMRI data enabled us to check whether our results agreed with previous findings, before examining probable fibre connections between active areas in each observer. We modelled rivalry alternations from their reported onset to their reported offset in each alternation direction and tested in which brain areas these two time courses accounted for the variability in the data acquired during rivalry viewing. In other words, our event-related analysis tested whether the measured time-series data in each voxel could be predicted by a time course that consisted of a response to each reported perceptual alternation from the red to the green grating and that was constant otherwise, and by a corresponding time course for alternations from the green to the red grating. The question was which voxels in the brain responded to rivalry alternations during ongoing rivalry perception.

Many brain regions in all three participants exhibited BOLD signal changes that consistently followed reported rivalry alternations (test of conjunction null), $t(949)=2.93$, $p<0.05$, corrected for multiple comparisons by controlling the false discovery rate (FDR; 5% of voxels expected to be false positives; see Fig. 3). To clarify, significant voxels showed transient BOLD signal increases above the height threshold in each participant. In the left hemisphere, such signal changes occurred mainly in the inferior parietal lobule and extended into the sensorimotor cortex, including the likely location of right-hand finger representations. Other alternation-related signal

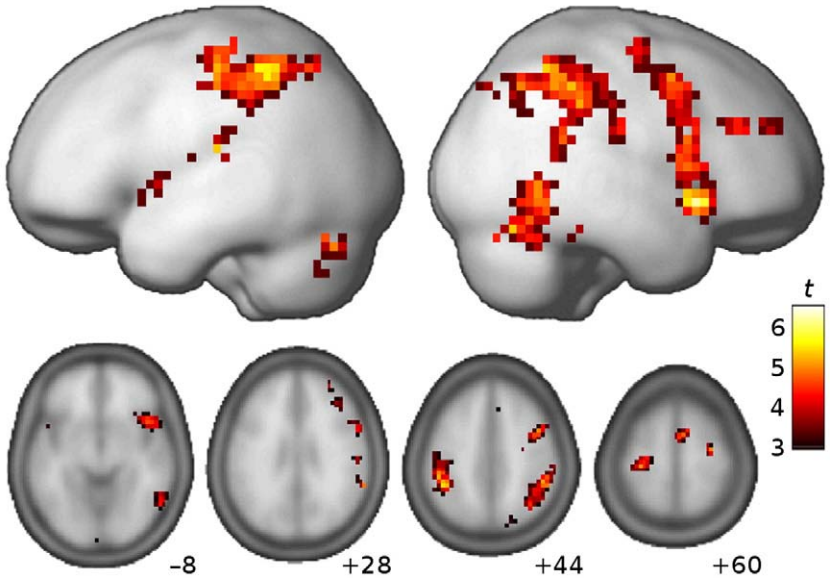

Fig. 3 – Brain areas with transient BOLD signal increases associated with reported binocular rivalry alternations in each participant. The results of a conjunction analysis ($t[949]=2.93$, $p<0.05$, FDR corrected) are superimposed on the ICBM-152 T_1 template (top row: within 20 mm of the brain surface). Some of the above-threshold clusters shown on the axial slices are in the right insula and inferior temporal gyrus (z=-8 mm), in the right middle and inferior frontal gyri (z=+28 mm), in the right precentral gyrus and the inferior parietal lobule bilaterally (z=+44 mm), and in the supplementary motor area (z=+60 mm).

Author's personal copy

changes that were consistent with the preparation and execution of key presses were located in the supplementary motor area and the cerebellum. In the right hemisphere, there was a cluster in the posterior part of the inferior temporal gyrus and surrounding tissue. We also found clusters of event-related signal changes in the right hemisphere in the inferior parietal lobule, including the angular and supramarginal gyri; in the precentral gyrus, the opercular part of the inferior frontal gyrus, and the insula; and in the middle frontal gyrus. Similar activity patterns have been reported in other whole-brain fMRI studies of binocular rivalry alternations (Lumer et al., 1998; Lumer and Rees, 1999) and for spontaneous alternations in other forms of visual bistable perception (e.g., Ilg et al., 2008; Kleinschmidt et al., 2002; Sterzer et al., 2002; Sterzer and Kleinschmidt, 2007). We found no transient signal decreases time-locked to reported rivalry alternations in the group analysis.

2.2.3. *Tractography*

Based on the BOLD signal maxima associated with reported rivalry alternations in each observer's right hemisphere, we created same-size masks as seeds and targets for probabilistic tractography. In addition to fulfilling the prespecified mask criteria (see Section 4.2.4.), all mask clusters survived an extent threshold of $p=0.001$, corrected, with the exception of a cluster in JM's middle temporal pole ($p=0.12$), one in GH's middle frontal gyrus ($p=0.09$), and one in her superior parietal lobule ($p=0.009$). Even in these three masks, all voxels survived a height threshold of $p=0.01$, FDR corrected. Application of the mask criteria led to at least three frontal, two parietal, and three temporal or occipital masks in each observer. Common mask locations included the middle or inferior frontal gyrus, the precentral gyrus, the inferior parietal lobule, and the posterior temporal lobe.

An overview of mask locations and detected probabilistic connections is given in Fig. 4 and Table 2. The degree of structural connectivity between masks was moderate in JM and high in VN and GH, with almost all masks connected with each other either directly or via other masks. Yet connection probabilities tended to be low: The highest percentage of streamline samples that reached their target mask from any one seed voxel was 6.8% (340.8 samples out of 5000); the highest percentage of such samples from all successful seed voxels in a cluster was 1.8% (1081.8 samples out of 12.2×5000; all values from JM's tract 1). We address this issue in the discussion.

There were obvious interindividual differences in the exact location of masks and the probability of fibre connections between them. In VN early visual areas were linked to later ones in the ventral and dorsal stream. Frontal masks were well-connected to each other and were linked to parietal (and occipital) masks most strongly through a mask in the inferior frontal gyrus. In JM parietal and middle temporal masks were well-connected to each other and to the temporal pole. In GH the strongest connections were between two frontal masks and between a mask in the rolandic operculum and one in the posterior part of the superior temporal gyrus. In spite of the differences, there was one connection among the three most-probable connections in each observer that linked posterior and anterior masks by following a section of the inferior occipitofrontal fasciculus (i.e., tract 3 in all observers).

3. Discussion

The aim of our two experiments was to learn more about both the cortical activity during binocular rivalry and its underlying structural connectivity. The comparison of rivalry perception with binocular-fusion perception in Experiment 1 yielded a higher BOLD signal during rivalry in right frontal, parietal, and occipital areas, among others. The increased activity can be explained neither by visual competition in the comparison condition nor by confounds from motor reports or from the difficulty of judgements, because none of these factors existed in our experiment. Using probabilistic diffusion tractography in Experiment 2, we found that almost all right-hemispheric regions with rivalry-alternation-related BOLD signal were connected to each other either directly or indirectly by probable anatomical pathways. Our results also suggest that alternation-related information might travel along the inferior occipitofrontal fasciculus between posterior and frontal areas.

One limitation of our experiments is the small number of participants, six in Experiment 1 and three in Experiment 2. We can conclude from the strong fixed-effects group results in Experiment 1 that at least our particular participants showed a mean increased BOLD signal in right frontal, parietal, and occipital areas during rivalry viewing compared to fusion viewing. In addition, random-effects group results, including effect sizes with standard errors, indicate that the finding might generalise to the population. The conjunction analysis in Experiment 2 served to support the tractography findings by showing that the identified BOLD signal changes in each participant, which formed the basis of individuals' seed and target masks, were those commonly reported in the literature. Despite the presented support, it has not been established beyond doubt that the results of our two experiments generalise to the population; yet they do provide promising bases for future investigations into the neural bases of perceptual consciousness and binocular rivalry.

3.1. *Brain areas associated with binocular rivalry*

The conscious experience of rivalry viewing in Experiment 1 was similar to that of fusion viewing; in fact, some of the observers were surprised when told that, during rivalry blocks, they had been shown dissimilar stimuli simultaneously. However, rivalry viewing typically includes perceptual alternations, which only one observer did not confirm. During these periods of mixed rivalry perception, observers saw parts of two orthogonal gratings rotate instead of seeing one grating rotate. Insofar as other factors, such as attention, were associated with this perceptual difference and influenced the BOLD signal of the corresponding 30-s blocks, we cannot exclude their contribution to our results. Frontoparietal activity is commonly found to be associated with changes in the contents of visual awareness (Rees, 2007), yet it is currently unknown what contribution attention makes to this finding. As spontaneous perceptual alternations of bistable stimuli occur even in the absence of attention to the stimuli

Author's personal copy

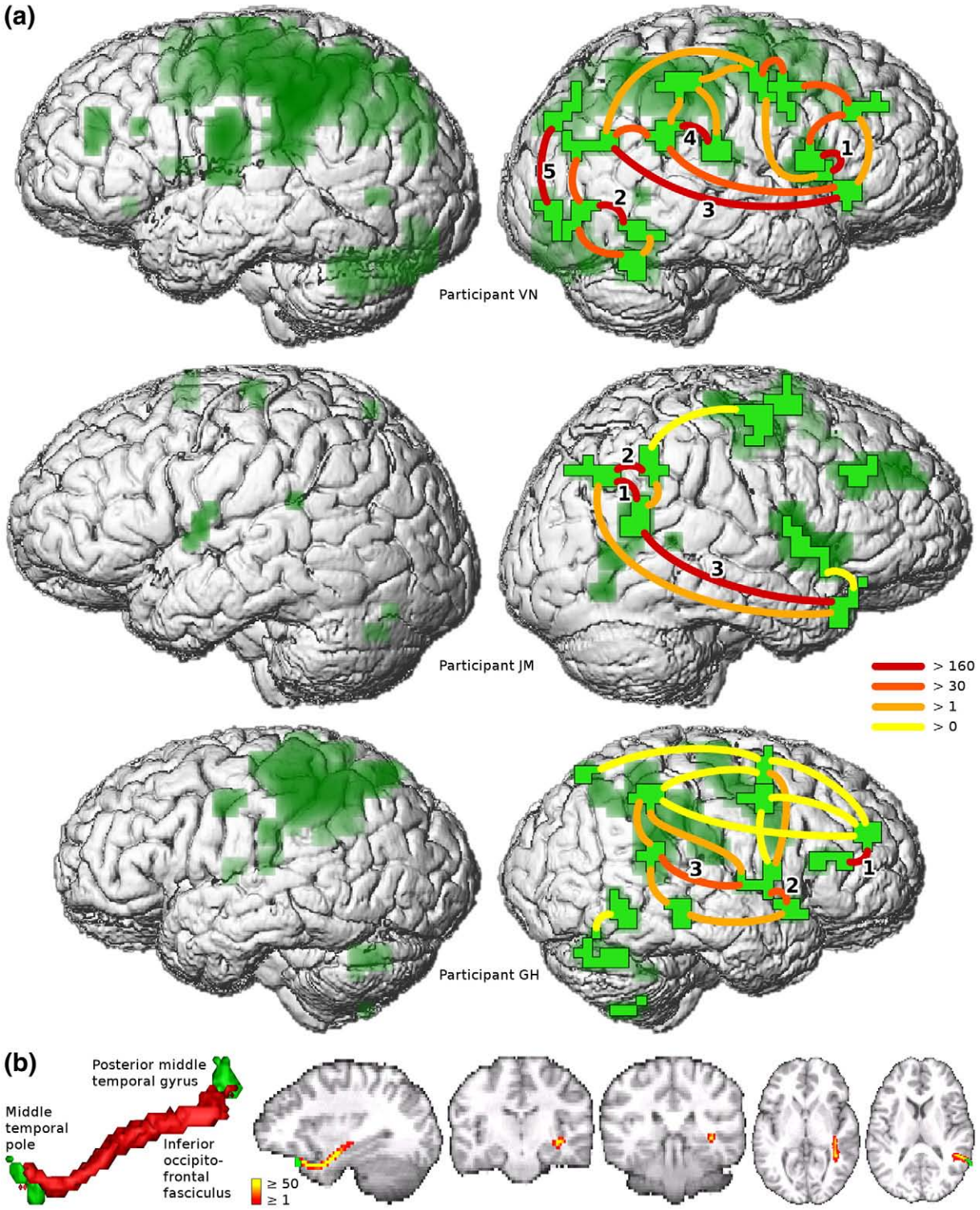

Fig. 4 – Probabilistic white matter fibre tracts between areas associated with reported binocular rivalry alternations. (a) Green areas show alternation-related BOLD signal in three observers (top row: VN, $t[348]=5.06$, $p<0.01$; middle row: JM, $t[261]=4.71$, $p<0.05$; bottom row: GH, $t[340]=5.03$, $p<0.01$, each FWE corrected), within 40 mm of the brain surface and superimposed on their surface-rendered structural data. Probabilistic fibre tracts between bright green seed and target masks in the right hemispheres are displayed schematically, with hotter colours showing greater numbers of seeded streamline samples reaching their target (numbers of the stronger direction; 26 tracts with fewer successful samples are omitted in VN). Details of numbered tracts are given in Table 2. (b) As an example, JM's tract 3 is shown as a three-dimensional rendering and as the number of successful streamline samples per voxel superimposed on his structural data.

Author's personal copy

Table 2 – Example tracts between right-hemispheric clusters associated with reported binocular rivalry alternations.

Tract	Cluster maximum					Voxels with tracts (SE)	Samples	
	Anatomical label	x	y	z	t		Max. (SE)	Total (SE)
VN								
1	Insula	35	22	4	5.70	73.4 (0.9)	85.4 (7.2)	766.9 (40.8)
	Inferior frontal gyrus, opercular part	59	15	9	7.72	47.8 (1.9)	140.8 (15.9)	633.2 (79.4)
2	Inferior temporal gyrus	63	-55	-20	6.31	17.6 (1.1)	79.6 (8.4)	257.6 (22.2)
	Inferior occipital gyrus	42	-75	-3	5.22	24.6 (1.5)	32.4 (8.1)	105.0 (19.6)
3	Middle occipital gyrus	34	-80	26	5.58	52.0 (3.8)	38.2 (8.0)	241.3 (57.7)
	Inferior frontal gyrus, orbital part[a]	31	28	-11	5.41	3.0 (0.8)	2.8 (0.6)	5.0 (1.6)
4	Rolandic operculum	55	-22	14	8.60	18.4 (0.9)	132.2 (20.5)	234.3 (27.8)
	Supramarginal gyrus	67	-44	26	7.90	18.4 (1.1)	39.2 (7.2)	131.8 (12.8)
5	Calcarine fissure and surrounding cortex	13	-89	-1	7.48	43.4 (1.2)	37.4 (8.1)	199.0 (38.0)
	Cuneus	13	-82	41	5.95	11.2 (0.7)	13.4 (1.1)	50.8 (4.0)
JM								
1	Angular gyrus	45	-63	36	4.90	54.4 (2.0)	141.0 (25.1)	1716.4 (221.0)
	Middle temporal gyrus	70	-54	16	6.12	12.2 (0.5)	340.8 (21.7)	1081.8 (56.5)
2	Supramarginal gyrus	57	-44	38	4.95	22.2 (0.9)	36.6 (9.0)	162.4 (40.0)
	Angular gyrus	45	-63	36	4.90	11.0 (0.4)	2.4 (0.2)	14.3 (1.4)
3	Middle temporal gyrus	70	-54	16	6.12	7.0 (0.4)	63.4 (7.4)	171.6 (17.9)
	Middle temporal pole	38	22	-37	4.86	19.0 (2.3)	4.0 (0.7)	30.9 (6.2)
GH								
1	Inferior frontal gyrus, triangular part	65	32	5	5.52	30.6 (2.1)	307.2 (16.5)	668.2 (16.6)
	Middle frontal gyrus	31	51	18	5.03	38.6 (1.4)	133.4 (7.0)	309.5 (21.2)
2[b]	Rolandic operculum[c]	54	-4	-2	5.34	12.6 (0.5)	16.6 (1.9)	64.1 (9.5)
	Superior temporal pole	53	18	-19	5.80	6.8 (0.9)	3.0 (0.6)	11.7 (2.0)
3	Superior temporal gyrus	56	-42	17	7.52	21.4 (2.0)	9.4 (2.2)	53.7 (11.9)
	Rolandic operculum[c]	54	-4	-2	5.34	1.6 (0.7)	0.8 (0.4)	1.1 (0.7)

Tract numbers correspond to those in Fig. 4. Details of cluster maxima are in MNI space with coordinates in millimetres and *t* values based on individual fixed-effects analyses in VN, $t(348)=5.06$, $p<0.01$; JM, $t(261)=4.71$, $p<0.05$; and GH, $t(340)=5.03$, $p<0.01$, each FWE corrected. All other data are in diffusion space. Each of the 85 voxels in a cluster was seeded with 5000 streamline samples. Tracts between cluster pairs are characterised in both directions by the number of seed voxels with at least one sample reaching the target cluster, by the maximum number of samples reaching the target cluster from a single seed voxel, and by the total number of samples reaching the target cluster (means of five probabilistic tractography analyses). Connectivity values for cluster pairs do not necessarily match because of differences in encountered brain geometry when tracking fibres in the opposite direction. SE = standard error.

[a] We give values for a local maximum because the cluster maximum in the insula (see VN's tract 1) was farther from the tract.

[b] This tract is biologically unlikely because it crosses the Sylvian fissure laterally.

[c] The individual's structural data does not agree with the assigned AAL label *Superior temporal gyrus*.

(Pastukhov and Braun, 2007), future studies could investigate the neural activity of rivalry viewing under different amounts of attention using a dual-task design.

We expected the results from the comparison of rival and normal perception in Experiment 1 to differ from the findings of event-related rivalry studies, such as our Experiment 2, for four reasons: First, the former study identified areas with increased activity during ongoing rivalry perception, whereas the latter studies identified areas with transient activity increases time-locked to perceptual rivalry alternations. Second, Experiment 1 is the only neural comparison of rivalry with nonrival perception to date. Third, visual stimuli differed in attributes such as luminance, colour, and rotation speed, affecting in particular the respective visual areas. Fourth, observers in our Experiment 1 did not report their perception. Conversely, Experiment 2's results include effects related to the reporting of perceptual alternations, for lack of realistic nonrival simulations of rivalry alternations. We accepted the inclusion of these well-known effects because it allowed us to check that our single-subject tractography analyses were based on fMRI results that are consistent with previous studies.

The results of our two studies clearly differed in the occipital lobe, in the supplementary motor area, and in the left hemisphere. There were some similarities in the right frontal and parietal lobes, but the superior parietal and the two frontal clusters that were more activated during rivalry than during fusion overlapped rivalry-alternation clusters only at a more liberal statistical threshold. Similarly, the locations of ongoing-rivalry maxima were different from Lumer et al.'s (1998) rivalry-alternation results and, as predicted, also from those of comparisons with permanent suppression conditions (Lumer et al., 1998; Lumer and Rees, 1999), with the exception of the superior parietal region discussed next.

The right superior parietal lobule, which showed increased activity during rivalry viewing as compared to fusion viewing, has been found to be associated with binocular rivalry alternations (Lumer et al., 1998; Lumer and Rees, 1999) and with changes in visual awareness more generally (Naghavi and Nyberg, 2005; Rees et al., 2002; Rees, 2007). However, the parietal activity during ongoing-rivalry perception in our Experiment 1 was located more medially than the parietal activity associated with rivalry alternations in our Experiment

Author's personal copy

2, suggesting that neighbouring regions might be involved in the different components of binocular rivalry. Work on the exact role of specific parietal (and frontal) regions in bistable perception is now underway in several research groups. A first result is that activity in the anterior intraparietal sulcus increases with the degree of perceptual incongruence of a slant rivalry stimulus (Brouwer et al., 2009). This is in line with our finding of ongoing-rivalry activity in a section of the intraparietal sulcus (as part of the superior parietal cluster, which extended into the inferior parietal lobule), because the binocular rivalry stimuli were perceptually incongruent whereas the binocular fusion stimuli were congruent.

Our ongoing-rivalry results in Experiment 1 differed from rivalry-alternation results, yet they were consistent with some of Lumer and Rees's (1999) findings. The four maxima with the strongest effect of rivalry versus fusion were near a subset of activity maxima that these authors had identified as correlating with an early extrastriate indicator of rivalry alternations. Their study was similar to our Experiment 1 and different from both our Experiment 2 and Lumer et al.'s (1998) studies in the absence of motor reports and the analysis of ongoing rivalry perception. It is therefore plausible that the activity in the network of common regions, namely the superior occipital gyrus, the superior parietal lobule, and the precentral and middle frontal gyri of the right hemisphere, is specific to ongoing rivalry perception rather than to the experience of rivalry alternations.

Neural activity was lateralised to the right hemisphere when we compared binocular rivalry to fusion. This was also the case for most of the frontal and temporal activity changes associated with rivalry alternations. The right lateralisation of frontoparietal activity is in line with previous reports of rivalry-related frontal activity only in the right hemisphere (Lumer and Rees, 1999) and unilateral alternation-related activity in the right inferior frontal gyrus and the right superior and inferior parietal lobules (Lumer et al., 1998). Yet we know that binocular rivalry can be processed independently in the left hemisphere, at least in split-brain observers (O'Shea and Corballis, 2001, 2005b). The hemispheric asymmetry normally observed in binocular rivalry could have to do with the visuospatial processing preference of the right hemisphere, which even extends to top-down influences of frontoparietal areas on visual cortex (Ruff et al., 2009) and possibly also to the resolution of visuospatial ambiguities (Corballis, 2003). The asymmetry could also be related to the right-hemispheric dominance of visual attention in several frontoparietal areas (Corbetta and Shulman, 2002; Kastner and Ungerleider, 2000; Nobre, 2001), as both bottom-up and top-down attention influence binocular rivalry (Blake and Logothetis, 2002; Tong et al., 2006). However, rivalry shares the overlap with attention-related frontoparietal areas with other changes in conscious perception (Naghavi and Nyberg, 2005; Rees et al., 2002), which is another reason why the right-hemispheric tendency is unlikely rivalry-specific.

3.2. *Anatomical networks in binocular rivalry*

Frontal, parietal, and temporal regions in the right hemisphere that are associated with reported binocular rivalry alternations seem to form not only a functional, but also an anatomical network. We were able to identify structural connections of at least low probability between all such regions in each participant, with the exception of two regions in one participant. Higher probability pathways between posterior and frontal alternation-related areas followed the inferior occipitofrontal fasciculus.

The variability in mask locations in our three observers makes generalisations somewhat difficult. Interindividual differences in the location of masks could, of course, be caused by actual differences in brain processing. However, some of them also arose because we could not include activity clusters in the tractography analyses if they were connected functionally to other clusters at the mask-size threshold. The smaller total number of masks in JM may have to do with his smaller number of scans, which the slightly more liberal statistical threshold for defining masks could only partially offset. The between-subject differences in mask location notwithstanding, the alternation activity present in all three observers was in good accordance with previous fMRI findings of binocular rivalry (Lumer et al., 1998; Lumer and Rees, 1999) and bistable perception (e.g., Ilg et al., 2008; Kleinschmidt et al., 2002; Sterzer et al., 2002; Sterzer and Kleinschmidt, 2007).

Diffusion data allow inferences about the orientation of fibre tracts, but not about the direction of information flow in these pathways, nor about their actual use for communication in a particular task. The low connection probabilities reported here illustrate additional challenges in the interpretation of results from probabilistic tractography analyses. The proportion of streamline samples reaching the target cluster from a seed voxel depends not only on the existence of an anatomical connection, but also on such factors as the data quality, voxel size, diffusion model, tract size, changes in the direction of the tract, diverging, branching, other fibre bundles, and the distance between seed and target (as each voxel contains uncertainty in the fibre orientations). This means that connectivity values are not necessarily high even for well-established pathways. For example, Bridge et al. (2008) reported that only 0.8% of the samples seeded in the lateral geniculate nucleus reached an early visual mask. The above factors make it difficult to interpret the reported posterior probabilities of connections as presence or absence of anatomical links (Bridge et al., 2008; Johansen-Berg and Behrens, 2006), and there are currently no statistical significance tests for tractography pathways (Aron et al., 2007). However, because probabilistic tracts follow diffusion directions, which indicate fibre orientations, tracts with a higher number of successful streamline samples are more promising candidates for further investigation than those with very few or no successful samples. The present results are thus a first survey of fibre bundles that might play a role in binocular rivalry.

Despite the discussed limitations, probabilistic tractography analyses enabled us to detect potential anatomical pathways between cortical regions associated with reported binocular rivalry alternations in human observers. This was possible only because we could track fibres in grey matter and in areas of crossing fibres based on in vivo and noninvasive brain diffusion data. Overall, the identified probabilistic fibre tracts between alternation-related regions could be the anatomical basis for their hypothesised functional and

Author's personal copy

effective connectivity. Our results also suggest that the inferior occipitofrontal fasciculus could be involved in communicating information between posterior and frontal areas during binocular rivalry alternations.

Taken together, our tractography results are an encouraging first step toward understanding the structural network that is the basis for binocular rivalry. We focused on fibre tracts between areas associated with reported perceptual alternations during rivalry, which was an extension of previous work on the location of such activity (Lumer et al., 1998; Lumer and Rees, 1999). Our results fit well with two major neurobiological theories of consciousness. The structural connectivity between visual and higher areas active during changes in visual awareness, which we identified in individual observers, could mediate the widespread recurrent interactions that Lamme's (2003, 2006) theory requires for consciously accessible perception. Interconnectivity is also necessary for attentional amplification and hence conscious access to visual information according to Dehaene and colleagues (Dehaene and Naccache, 2001; Dehaene et al., 2006); the inferior occipitofrontal fasciculus in particular might be an important long-distance connection in their hypothesised global neuronal workspace. We hope that future investigations of the involvement of specific tracts in conscious perception, and particularly in binocular rivalry, will benefit from a more mature knowledge of the relevant cortical regions and their contributions.

3.3. *Conclusion*

Our findings suggest the following conclusions: Ongoing binocular rivalry perception differs from normal human vision, characterised by binocular fusion, in increased neural activity in right frontal, parietal, and occipital regions. The locations of activity foci also differ from those found in comparisons of rivalry with permanent suppression, supporting the distinction between these two comparison conditions for rivalry. An exception to the differing patterns of cortical activity are adjacent activity locations in the right parietal lobule, which also contains activity associated with perceptual alternations and thus seems to accommodate several rivalry-related functions in close proximity. Most regions in the right hemisphere that are associated with reported rivalry alternations are linked by probabilistic fibre tracts, some of which follow long-distance connections such as the inferior occipitofrontal fasciculus. The corresponding anatomical networks might mediate communication within the functional networks related to changes in conscious perception during binocular rivalry.

4. Experimental procedures

4.1. *Experiment 1*

4.1.1. *Participants*

Six volunteers aged between 20 and 32 years (M=27.0 years, two females, one left-handed) participated in Experiment 1 in exchange for images of their brains. Their vision was normal or corrected-to-normal by adjusting the scanner binoculars. All observers gave written informed consent for participation in the study, which had approval from the New Zealand Upper South A Ethics Committee.

4.1.2. *Apparatus*

We created still versions of the stimuli in MATLAB 7.4 and double animations using Microsoft Visual C# 2005 with Microsoft DirectX 9.0c for hardware acceleration. Stimuli were presented in adjustable binocular glasses (Avotec SV-7021, Stuart, FL) from a Pentium 4 computer (3.4 GHz, 1 GB of RAM). We measured the luminance of stimulus components with a Nuclear Associates Precision Photometer (model 07-621, Carle Place, NY).

A Signa HDx 3 T MRI scanner (GE Healthcare Technologies, Waukesha, WI) with an 8-channel brain coil served to collect imaging data at the Van der Veer Institute for Parkinson's and Brain Research in Christchurch, New Zealand. We used head restraint straps or soft pads to help reduce head motion, in addition to instructions to keep the head as still as possible.

4.1.3. *Stimuli and procedure*

The binocular-rivalry stimuli consisted of a square-wave grating presented to the left eye of the observer and an otherwise identical grating of orthogonal orientation presented to the right eye (see Fig. 1). Gratings had a spatial frequency of approximately 0.5 cycles per degree of visual angle.[1] Each grating was shown within an annular window (3.9° to 11.9°), smoothed with a Gaussian (SD=0.4°), on a black background (luminance=0.6 cd/m^2). Both gratings were surrounded by a gap (≥1.5°) and then an identical pattern of small white (120.6 cd/m^2) square contours (0.4°), modelled after van Ee's (2005) Fig. 1. These dioptic contours and the central white fixation points (0.1°) helped to maintain stable alignment of the left and right eye's view. Gratings were black and green (16.5 cd/m^2) and rotated clockwise at 0.25 Hz around the fixation points. In the binocular-fusion stimuli display, gratings were identical in orientation.

We instructed observers to look at the fixation point during each of the two to three experimental runs. Runs lasted 5 min and consisted of continuously alternating 30-s blocks of the fusion and rivalry conditions, with the starting condition assigned randomly to observers.

4.1.4. *Data acquisition and analysis*

During each experimental run, we obtained 100 whole-brain T_2*-weighted two-dimensional echo-planar gradient-recalled image volumes (repetition time [TR]=3000 ms; echo time [TE]=35 ms; flip angle [FA]=90°; contiguous, interleaved axial slices; slice thickness=4 mm; field of view [FOV]=240 mm; image matrix=64×64; in-plane resolution=3.75×3.75 mm^2), excluding the initial 12 s of data, which were discarded to allow for stabilisation of the magnetic resonance signal. For better spatial registration and localisation of activity, we also acquired a high-resolution anatomical whole-brain image

[1] We give visual angles as approximations based on the manufacturer's specifications because the distance between the eye and the scanner binoculars changed with head size. The distance between a male participant's eyes and the binoculars was 1.5 cm.

Author's personal copy

volume, using a T_1-weighted three-dimensional inversion recovery gradient-recalled pulse sequence (inversion time [TI] = 400 ms; TR = 6.3 ms; TE = 2.8 ms; FA = 15°; contiguous axial slices; slice thickness = 1 mm; FOV = 240 mm; before zero-filling: image matrix = 256 × 256; in-plane resolution = 0.94 × 0.94 mm^2).

Functional and structural imaging data were analysed with SPM5 (http://www.fil.ion.ucl.ac.uk/spm/software/spm5/) in MATLAB 7.4. We performed the following preprocessing steps: We spatially realigned the functional images to remove movement artefacts and then coregistered the structural image to the functional images. During segmentation of the structural image, we estimated spatial normalisation parameters and obtained a bias-corrected version of the image. To facilitate a group analysis in Montreal Neurological Institute (MNI) space, we normalised the structural and functional images and spatially smoothed the latter with a Gaussian kernel of 8 mm full width at half maximum. General linear models were used for mass-univariate analyses of the preprocessed fMRI data. This involved fitting data with a linear combination of the regressors in the design matrix, in order to obtain estimates of the relative contribution of each regressor to the time series data at each voxel.

The mixed-effects analysis of Experiment 1's block-design data proceeded in two stages. We first performed a fixed-effects analysis of each observer's preprocessed data. The design matrix contained eight regressors per run: a regressor for the rivalry condition, a global mean signal regressor, and the six spatial realignment parameters for modelling residual movement-related artefacts. We modelled changes in brain activity during the alternating 30-s blocks by convolving a series of boxcar functions with the canonical haemodynamic response function (HRF) implemented in SPM5. To test which voxels in the brain were more activated in the rivalry condition than in the fusion condition, we constructed a contrast for each observer with positive weights for the rivalry parameter estimates so that the sum of the weights across the runs was +1. The contrasts from all observers were then entered into a random-effects analysis at the second stage, which tested the null hypothesis that the contrasts are zero with a one-sample *t* test. This analysis allows population inferences about brain regions associated with rivalry as opposed to fusion.

All reported statistical thresholds are height thresholds (*t* values) for voxel-level inferences unless stated otherwise, in which case they are extent thresholds (numbers of voxels) for cluster-level inferences. Reported significance probabilities (*p* values) refer to one-tailed *t* tests. We labeled cluster maxima using Anatomical Automatic Labeling (Tzourio-Mazoyer et al., 2002).

4.2. *Experiment 2*

Only experimental-procedure details that differ from those in Experiment 1 are described here.

4.2.1. *Participants*

The three right-handed observers who participated in Experiment 2 were 29-year-old male VN, 20-year-old male JM, and 26-year-old female GH. Two of the observers, VN and GH, attended a training session in which they saw the rivalry stimuli in a head-mounted display and pressed keys on a keyboard to report their perception; JM observed the rivalry display in Experiment 1 and practised key responses for several minutes before scanning. The data of two additional observers were excluded from the analyses, one's because of excessive mixed perception (50% of the scanning time) and the other's because of too-brief periods of uninterrupted exclusive visibility (M = 2.8 s).

4.2.2. *Apparatus*

A standard two-key response box linked to the presentation computer was used to record participants' responses.

4.2.3. *Stimuli and procedure*

In this experiment, we presented only binocular-rivalry stimuli. We increased the rotation speed of the gratings to 1 Hz, and we decreased and adjusted their luminances separately for each eye so that they appeared of similar intensity to the observer. We took these measures to try to lengthen and balance periods of exclusive visibility. The stimuli were similar to those described by Haynes et al. (2005) and Haynes and Rees (2005), which had been designed to elicit long exclusive and short mixed perception. Additionally, one of the gratings was black and red (M = 1.5 cd/m^2) and the other black and green (M = 2.5 cd/m^2) to facilitate the reporting of rivalry alternations. Even though the colour-eye assignments were random, the three observers whose data were included in the analyses viewed the red grating with their left eyes.

Participants observed the rivalry stimuli in the scanner for a total of 20 min (VN, GH) or 15 min (JM), split into three to five runs. They were instructed to look at the fixation point and to report periods of exclusive visibility of the red and the green grating by holding down one of two keys on the response box in their right hands; when they saw parts of both gratings, they were to hold down both keys.

4.2.4. *Data acquisition and analysis*

In addition to the functional and structural imaging as described for Experiment 1 (except 80 instead of 100 functional images in GH's 4-min runs), we took diffusion-weighted images of the whole brain with a two-dimensional echo-planar spin-echo pulse sequence (TR = 13 000 ms; TE = 75.5 ms; FA = 90°; contiguous axial slices; slice thickness = 3 mm; FOV = 240 mm; before zero-filling: image matrix = 128 × 128; in-plane resolution = 1.88 × 1.88 mm^2; after zero-filling down-sampled to this resolution using a custom-written MATLAB function). We performed diffusion weighting along 28 independent directions (b = 1000 s/mm^2) and also acquired four reference images (b = 0).

Before performing the other preprocessing steps, we corrected for differences in the acquisition time of functional slices. The design matrix in the fixed-effects analyses of each observer's event-related data contained nine regressors per run: a regressor for reported rivalry alternations from the red to the green grating, a regressor for reported alternations in the opposite direction, a global mean signal regressor, and the six spatial realignment parameters for modelling residual movement-related artefacts. We modelled changes in brain activity related to perceptual alternations by convolving a

Author's personal copy

series of boxcar functions, which were +1 from the reported onset of an alternation period to its reported offset and 0 elsewhere, with the canonical HRF implemented in SPM5. The regressors, including these two HRF-convolved event time courses, were fitted to the measured data. The aim of the choice of stimuli characteristics was to obtain perceptual alternation rates that balanced the number of measured events with signal loss due to the low-pass filtration of the HRF. To allow for a group-based comparison of our results with previous event-related fMRI findings, we performed a conjunction analysis of the preprocessed data, which allows inferences about the effects that are present in each of the three observers.

To probe for white matter connections between areas related to rivalry alternations, we performed the same analysis of the functional data separately for each observer without the normalisation step. We created masks for BOLD signal maxima that were more than 12 mm apart and that survived a height threshold of $p<0.01$, FWE corrected, in VN and GH ($t[348]=5.06$ and $t[340]=5.03$, respectively) and $p<0.05$, FWE corrected, in JM ($t[261]=4.71$), from whom we had fewer imaging data. For diffusion tractography results to be comparable, all seed masks need to be the same size, as do all target masks. The masks we created consisted of the 16 voxels (900 mm^3) with the highest t values that included one of the selected maxima; mask voxels were connected with each other at the relevant statistical threshold, but separate from other masks. The size of the masks was aimed at capturing the anatomical pathways arriving at or leaving a region while including only the functionally most relevant voxels. We excluded left-hemispheric clusters for three reasons. First, we expected stronger confounds from right-hand key presses in the left hemisphere. Second, we expected more rivalry-related activity in the right hemisphere based on previous findings (e.g., Experiment 1; Lumer et al., 1998; Lumer and Rees, 1999). Third, we found that the distributions of above-threshold BOLD signal in the left hemispheres tended to be unsuitable for creating several separate masks (see Fig. 4). The clusters were saved as mask images using MarsBaR 0.41 (http://marsbar.sourceforge.net/).

Diffusion-weighted data were processed with analysis tools in FSL 4.1 (Smith et al., 2004). We used FDT 2.0 (Behrens et al., 2003) to correct for head motion and distortions from eddy currents in the gradient coils. Markov Chain Monte Carlo sampling was then run to build up posterior probability distributions on local diffusion parameters, which included two fibre orientations in each voxel if supported by the data (Behrens et al., 2007). FLIRT 5.5 (Jenkinson and Smith, 2001) served to obtain the required transformation matrices by registering functional and diffusion images to the structural image, itself registered to the ICBM-152 T_1 standard brain template. After we transformed the mask images from functional into diffusion space, we thresholded them individually to restore each cluster's volume. Probabilistic fibre tracking consisted of repeatedly sampling the distributions at each voxel to generate streamlines through the diffusion data. We initiated 5000 streamline samples from each of the 85 voxels in a particular seed mask, with a pathway step length of 0.5 mm, a curvature threshold of 0.2 (angle between successive pathway steps at least ±80°), and all other cluster masks as classification targets. We performed local parameter estimation and tractography between all cluster mask pairs in both directions five times per observer and report the respective mean results here.

Acknowledgments

This research was supported by the Van der Veer Institute for Parkinson's and Brain Research and the Canterbury Medical Research Foundation, New Zealand.

Appendix A. Supplementary data

Supplementary data associated with this article can be found, in the online version, at doi:10.1016/j.brainres.2009.09.080.

REFERENCES

Aron, A.R., Behrens, T.E.J., Smith, S., Frank, M.J., Poldrack, R.A., 2007. Triangulating a cognitive control network using diffusion-weighted magnetic resonance imaging (MRI) and functional MRI. J. Neurosci. 27, 3743–3752.

Behrens, T.E.J., Woolrich, M.W., Jenkinson, M., Johansen-Berg, H., Nunes, R.G., Clare, S., et al., 2003. Characterization and propagation of uncertainty in diffusion-weighted MR imaging. Magn. Reson. Med. 50, 1077–1088.

Behrens, T.E.J., Johansen-Berg, H., Jbabdi, S., Rushworth, M.F.S., Woolrich, M.W., 2007. Probabilistic diffusion tractography with multiple fibre orientations: what can we gain? NeuroImage 23, 144–155.

Blake, R., Logothetis, N.K., 2002. Visual competition. Nat. Rev. Neurosci. 3, 1–11.

Bridge, H., Thomas, O., Jbabdi, S., Cowey, A., 2008. Changes in connectivity after visual cortical brain damage underlie altered visual function. Brain 131, 1433–1444.

Brouwer, G.J., Tong, F., Hagoort, P., van Ee, R., 2009. Perceptual incongruence influences bistability and cortical activation. PLoS ONE 4, e5056.

Corballis, P.M., 2003. Visuospatial processing and the right-hemisphere interpreter. Brain Cogn. 53, 171–176.

Corbetta, M., Shulman, G.L., 2002. Control of goal-directed and stimulus-driven attention in the brain. Nat. Rev. Neurosci. 3, 201–215.

Crick, F., Koch, C., 1990. Towards a neurobiological theory of consciousness. Semin. Neurosci. 2, 263–275.

Crick, F., Koch, C., 1998. Consciousness and neuroscience. Cereb. Cortex 8, 97–107.

Dehaene, S., Naccache, L., 2001. Towards a cognitive neuroscience of consciousness: basic evidence and a workspace framework. Cognition 79, 1–37.

Dehaene, S., Changeux, J.-P., Naccache, L., Sackur, J., Sergent, C., 2006. Conscious, preconscious, and subliminal processing: a testable taxonomy. Trends Cogn. Sci. 10, 204–211.

Haynes, J.-D., Rees, G., 2005. Predicting the stream of consciousness from activity in human visual cortex. Curr. Biol. 15, 1301–1307.

Haynes, J.-D., Deichmann, R., Rees, G., 2005. Eye-specific effects of binocular rivalry in the human lateral geniculate nucleus. Nature 438, 496–499.

Hering, E., 1964. Outlines of a Theory of the Light Sense. L.M.

Author's personal copy

Hurvich, D. Jameson, trans. (original work published 1874). Harvard University Press, Cambridge, MA.
Ilg, R., Wohlschläger, A.M., Burazanis, S., Wöller, A., Nunnemann, S., Mühlau, M., 2008. Neural correlates of spontaneous percept switches in ambiguous stimuli: an event-related functional magnetic resonance imaging study. Eur. J. Neurosci. 28, 2325–2332.
Jenkinson, M., Smith, S.M., 2001. A global optimisation method for robust affine registration of brain images. Med. Image Anal. 5, 143–156.
Johansen-Berg, H., Behrens, T.E.J., 2006. Just pretty pictures? What diffusion tractography can add in clinical neuroscience. Curr. Opin. Neurol. 19, 379–385.
Kastner, S., Ungerleider, L.G., 2000. Mechanisms of visual attention in the human cortex. Annu. Rev. Neurosci. 23, 315–341.
Kleinschmidt, A., Thilo, K.V., Büchel, C., Gresty, M.A., Bronstein, A.M., Frackowiak, R.S.J., 2002. Neural correlates of visual-motion perception as object- or self-motion. NeuroImage 16, 873–882.
Lamme, V.A.F., 2003. Why visual attention and awareness are different. Trends Cogn. Sci. 7, 12–18.
Lamme, V.A.F., 2006. Towards a true neural stance on consciousness. Trends Cogn. Sci. 10, 494–501.
Lee, S.-H., Blake, R., Heeger, D.J., 2005. Traveling waves of activity in primary visual cortex during binocular rivalry. Nat. Neurosci. 8, 22–23.
Lumer, E.D., Rees, G., 1999. Covariation of activity in visual and prefrontal cortex associated with subjective visual perception. PNAS 96, 1669–1673.
Lumer, E.D., Friston, K.J., Rees, G., 1998. Neural correlates of perceptual rivalry in the human brain. Science 280, 1930–1934.
Naghavi, H.R., Nyberg, L., 2005. Common fronto-parietal activity in attention, memory, and consciousness: shared demands on integration? Conscious Cogn. 14, 390–425.
Nobre, A.C., 2001. The attentive homunculus: now you see it, now you don't. Neurosci. Biobehav. Rev. 25, 477–496.
Ooi, T.L., Loop, M.S., 1994. Visual suppression and its effect upon color and luminance sensitivity. Vis. Res. 34, 2997–3003.
O'Shea, R.P., Corballis, P.M., 2001. Binocular rivalry between complex stimuli in split-brain observers. Brain Mind 2, 151–160.
O'Shea, R.P., Corballis, P.M., 2005a. Binocular rivalry in the divided brain. In: Alais, D., Blake, R. (Eds.), Binocular Rivalry. MIT Press, Cambridge, MA, pp. 301–315.
O'Shea, R.P., Corballis, P.M., 2005b. Visual grouping on binocular rivalry in a split-brain observer. Vis. Res. 45, 247–261.
Pastukhov, A., Braun, J., 2007. Perceptual reversals need no prompting by attention. J. Vis. 7, 1–17.
Polonsky, A., Blake, R., Braun, J., Heeger, D.J., 2000. Neuronal activity in human primary visual cortex correlates with perception during binocular rivalry. Nat. Neurosci. 3, 1153–1159.
Rees, G., 2007. Neural correlates of the contents of visual awareness in humans. Phil. Trans. Roy. Soc. Lond. B 362, 877–886.
Rees, G., Kreiman, G., Koch, C., 2002. Neural correlates of consciousness in humans. Nat. Rev. Neurosci. 3, 261–270.
Roser, M., Gazzaniga, M.S., 2004. Automatic brains – interpretive minds. Curr. Dir. Psychol. Sci. 13, 56–59.
Ruff, C.C., Blankenburg, F., Bjoertomt, O., Bestmann, S., Weiskopf, N., Driver, J., 2009. Hemispheric differences in frontal and parietal influences on human occipital cortex: direct confirmation with concurrent TMS-fMRI. J. Cogn. Neurosci. 21, 1146–1161.
Smith, S.M., Jenkinson, M., Woolrich, M.W., Beckmann, C.F., Behrens, T.E.J., Johansen-Berg, H., et al., 2004. Advances in functional and structural MR image analysis and implementation as FSL. NeuroImage 23, S208–S219.
Sterzer, P., Kleinschmidt, A., 2007. A neural basis for inference in perceptual ambiguity. PNAS 104, 323–328.
Sterzer, P., Rees, G., 2008. A neural basis for percept stabilization in binocular rivalry. J. Cogn. Neurosci. 20, 389–399.
Sterzer, P., Russ, M.O., Preibisch, C., Kleinschmidt, A., 2002. Neural correlates of spontaneous direction reversals in ambiguous apparent visual motion. NeuroImage 15, 908–916.
Tong, F., Engel, S.A., 2001. Interocular rivalry revealed in the human cortical blind-spot representation. Nature 411, 195–199.
Tong, F., Nakayama, K., Vaughan, J.T., Kanwisher, N., 1998. Binocular rivalry and visual awareness in human extrastriate cortex. Neuron 21, 753–759.
Tong, F., Meng, M., Blake, R., 2006. Neural bases of binocular rivalry. Trends Cogn. Sci. 10, 502–511.
Tzourio-Mazoyer, N., Landeau, B., Papathanassiou, D., Crivello, F., Etard, O., Delcroix, N., et al., 2002. Automated anatomical labeling of activations in SPM using a macroscopic anatomical parcellation of the MNI MRI single-subject brain. Neuroimage 15, 273–289.
van Ee, R., 2005. Dynamics of perceptual bi-stability for stereoscopic slant rivalry and a comparison with grating, house-face, and Necker cube rivalry. Vis. Res. 45, 29–40.
Wunderlich, K., Schneider, K.A., Kastner, S., 2005. Neural correlates of binocular rivalry in the human lateral geniculate nucleus. Nat. Neurosci. 8, 1595–1602.